Int. J. Multiphase Flow Vol. 18, No. 6, pp. 1077–1091, 1992
Printed in Great Britain.

0301-9322/92 $5.00 + 0.00

THE MOTION OF RIGID ROD-LIKE PARTICLES SUSPENDED IN NON-HOMOGENEOUS FLOW FIELDS

J. F. T. PITTMAN and N. KASIRI
Department of Chemical Engineering, University College of Swansea, University of Wales, Swansea SA2 8PP, Wales, U.K.

(Received 18 December 1991; in revised form 15 July 1992)

Abstract—Equations are written for the velocities of rotation and translation of rigid rod-like particles suspended in arbitrary Stokes flows. These make use of the first approximation from slender body theory for the evaluation of drag forces parallel and transverse to the particle axis, and neglect couples induced by shear stress at the particle surface. They are therefore asymptotically valid as the particle axis ratio becomes large. Simple forms of the equations, applying in constant viscosity flows, are solved, where possible analytically and otherwise numerically, and results obtained for particle motion in planar Poiseuille and sink flows. These are discussed and displayed in terms of appropriate dimensionless groups in a comprehensive set of plots, that can conveniently be used to provide information on translational and rotational velocities, and orientation and displacement as a function of time, including particle slip along and across streamlines, for a wide range of cases. In this way the effects of non-homogeneity in the flow fields are quantified.

Key Words: rod-like particles, particle mechanics, non-homogeneous flow fields, suspension mechanics, particle migration

INTRODUCTION

The motion of rod-like particles in flowing suspensions has been the subject of much work, both theoretical and experimental. Apart from its intrinsic particle mechanics interest, the topic has practical applications in the processing of fibre suspensions for the production of materials reinforced with short fibres, and elsewhere. In these technologies, the orientation and spatial distributions of particles influence product properties, and mathematical models relating these quantities to processing conditions—suspensions flow fields and so on—offer economic advantages in process design and optimization.

The starting point for the theoretical treatment of the low Reynolds number motion of rigid, neutrally buoyant particles is the solution by Jeffery (1922) for the motion of an ellipsoid in a homogeneous fluid field, i.e. one where velocity gradients are constant throughout the space occupied by the particle. Jeffery's equations were expressed in a more general form by Giesekus (1962) and Bretherton (1962) using a third rank shape tensor, and Brenner (1964) generalized the result to particles of arbitrary shape. For an ellipsoid of revolution (prolate or oblate spheroid) the shape tensor can be expressed in terms of the axis ratio, and Brenner's generalization means that Jeffery's equations of motion are valid for any axisymmetric particle, such as a square-ended rod or fibre, provided that an appropriate equivalent ellipsoid axis ratio is substituted.

Extensive experimental work, started by Taylor (1923) and continued by Mason and co-workers (Goldsmith & Mason 1967) and others, amply demonstrated the applicability of these equations. More recently, Jeffery's equations have formed the basis of a number of works seeking to predict fibre orientation during the flow and processing of fibre suspensions (e.g. Harris & Pittman 1976; Salariya & Pittman 1980; Givler *et al.* 1982; Gillespie *et al.* 1985; Vincent & Agassant 1985). They also underlie work developing constitutive equations for fibre suspensions (Dinh & Armstrong 1984; Lipscombe *et al.* 1988). Extensions to account for fibre–fibre interactions have been made by Folgar & Tucker (1984) and used to predict fibre alignment distributions in moulded parts (Jackson *et al.* 1984; Tucker 1984).

In all of these works the assumption that flow fields are homogeneous is retained, i.e. velocity gradients are taken to be constant throughout the region occupied by a particle. In many practical cases, however, this is not valid; for example, in injection or compression moulding using resins containing fibres, fibre length is often of the same order as part thickness, and velocity profiles during flow in the mould will show substantial variations of velocity gradient over a fibre length.

In some instances, polymer molecules in solution can be modelled as rigid rods, and their motion in non-homogeneous flow fields, specifically orientation distributions and migration along or across streamlines, is of considerable interest. Whilst the corresponding problem for flexible macro molecules has been addressed using the bead–spring model by, for example, Jhou (1985) and Brunn (1985), analyses of rigid rod motion in non-homogeneous flow fields have become available only in the last couple of years.

The present paper elaborates on the work of Kasiri (1988), where general equations for inertialess rotation and translation in arbitrary Stokes flows were derived, and solved analytically or numerically for a number of specific cases. Simultaneously, Shanker *et al.* (1990, 1991) were working independently in the same area. They obtained the same general equations, and applied them in one-dimensional planar shear flows. The emphasis in their work was on an investigation of the effects of non-homogeneous flow on the rheological properties of the supsension. In the work now described, the emphasis is, in contrast, on the motion of individual particles. The derivation of the general equations governing rotation and translation is briefly re-stated, with some additional comments. For the special case of constant viscosity flows, analytic results are obtainable for some simple cases. We consider one-dimensional planar shear flow and cylindrical sink or source flow, and derive expressions for angular and translational particle velocities. For the planar flow these are integrated analytically to give particle orientation and translation as functions of time; for the sink flow quadrature is necessary. Results are presented, in terms of appropriate dimensionless groups, that illustrate and quantify the effects of flow non-homogeneity on particle motion.

MOTION OF A ROD-LIKE PARTICLE IN A GENERAL STOKES FLOW

Consider a slender particle of characteristic radius R, neutrally buoyant in suspension. Identify a point on the particle axis by the co-ordinate l, with the origin at the particle centre, and $-L \leqslant l \leqslant L$. Express the instantaneous position of the point l by the position vector $\mathbf{x}(l)$ relative to a fixed Cartesian frame. Denote the undisturbed fluid velocity at position $\mathbf{x}$ by $\mathbf{v}(\mathbf{x})$ and the velocity of a point on the particle axis by $\mathbf{u}(l)$. As a consequence of the local relative velocity, $\mathbf{v}(l) - \mathbf{u}(l)$, the fluid exerts a force $\mathbf{f}(l)$ per unit length on the particle, and for conditions under which fluid inertia is negligible, slender body theory (Cox 1970) provides the following result:

$$\frac{\mathbf{f}(l)}{2\pi\mu} = \left[\frac{(\mathbf{v}-\mathbf{u})}{\ln\kappa} + \frac{\mathbf{a} + (\mathbf{v}-\mathbf{u})\ln\left(\dfrac{2\epsilon}{\lambda}\right)}{(\ln\kappa)^2}\right]\cdot[\mathbf{pp} - 2\mathbf{I}]$$

$$+ \frac{\frac{1}{2}(\mathbf{v}-\mathbf{u})}{(\ln\kappa)^2}\cdot[3\mathbf{pp} - 2\mathbf{I}] + O\left(\frac{1}{(\ln\kappa)^3}\right), \qquad [1]$$

where λ is a dimensionless measure of local particle radius, $\mathbf{I}$ is the identity tensor (Kronecker delta) and $\mathbf{p}$ is a unit vector directed in the positive l direction, tangential to the particle axis, and $\kappa = R/2L$. The vector $\mathbf{a}$ is given by

$$a_i(l) = \frac{1}{2}\left[\int_0^{l-\epsilon} + \int_{l+\epsilon}^{1}\right]\left(\frac{\delta_{ij}}{|\mathbf{x}-\mathbf{x}'|} + \frac{(x_i - x_i')(x_j - x_j')}{|\mathbf{x}-\mathbf{x}'|^3}\right)$$

$$\times (\delta_{jk} - \tfrac{1}{2}p_j p_k)(v_k(l') - u_k(l'))\,\mathrm{d}l'. \qquad [1a]$$

Here $\mathbf{x}$ denotes $\mathbf{x}(l)$ and $\mathbf{x}'$ denotes $\mathbf{x}(l')$, ϵ is arbitrary, $0 < \epsilon \ll 1$, and it can be shown that $\mathbf{f}(l)$ is independent of ϵ in the limit $\epsilon \to 0$. Equation [1] applies for a particle of any shape $\mathbf{x}(l)$, provided only that its radius of curvature at all points is not less than of order $2L$.

An important property of [1], for the present purposes, is that in the first approximation (the term in $1/\ln\kappa$) the local force and relative velocity are linearly related through a tensorial drag coefficient:

$$\mathbf{D} = D_\perp(\mathbf{I} - \mathbf{pp}) + D_\parallel \mathbf{pp},$$

where the coefficients associated with the components of the slip flow perpendicular and parallel to the particle axis are $D_\perp$ and $D_=$ and $D_= = \frac{1}{2}D_\perp = (2\pi\mu)/\ln\kappa$. This convenient representation no longer holds when terms in $(1/\ln\kappa)^2$ are included, because of the integration over particle length involved in evaluating **a**.

To simplify the subsequent working, and in common with Shanker *et al.* (1990), we therefore use only the first approximation, so that our results are strictly valid only asymptotically as the particle aspect ratio tends to infinity. Neglect of the second-order terms in the slender body result introduces a fractional error in **f** or order $|1/\ln\kappa|$; for example, for a typical fibre, as used in material reinforcement, with length 1 mm and diameter 10 μm, $|1/\ln\kappa| = 0.19$. This, however, forms a very conservative estimate of error in the results to be derived since, under the assumption of inertialess particle motion, absolute values of the drag coefficients are immaterial in the analysis.

Making the assumption of inertialess particle motion, we set the total force on the fibre to zero:

$$\mathbf{0} = \int_{-L}^{+L} \mathbf{f}(l)\,\mathrm{d}l = \int_{-L}^{+L} \mathbf{D}\cdot(\mathbf{v} - \mathbf{u}^{\mathrm{tr}} - \dot{\mathbf{p}}l)\,\mathrm{d}l. \qquad [2]$$

Here $\mathbf{u}(l)$ has been decomposed as

$$\mathbf{u}(l) = \mathbf{u}^{\mathrm{tr}} + \dot{\mathbf{p}}l \qquad [3]$$

and $\mathbf{u}^{\mathrm{tr}}$ is the translational velocity of the fibre centre.

When the radius of the particle is constant along its length, and the fluid viscosity is constant, then **D** is constant and it follows from [2] that

$$\mathbf{u}^{\mathrm{tr}} = \frac{1}{2L}\int_{-L}^{+L} \mathbf{v}\,\mathrm{d}l. \qquad [4]$$

This is the result for translational velocity, previously obtained by Shanker *et al.* (1990).

To obtain a result for angular velocity, consider the couple acting about the particle centre. This arises, in general, from two sources: the component of **f** due to a non-zero component of the relative velocity perpendicular to the fibre axis, and acting with lever arm l; and shear stress at the particle surface, due to that component of the relative velocity which is zero on the particle axis, and acting with a lever arm equal to the particle radius. The latter couple has been considered by Cox (1971) for a slender, straight, axisymmetric particle in a uniform shear flow, and an expression for the couple, denoted G'', acting on the particle as it lies along a streamline of this flow was derived for the case where the particle radius goes smoothly to zero at the ends. No analytic result could be obtained for blunt-ended bodies, such as chopped fibres, though Youngren & Acrivos (1975) obtained values of G'' from numerical solutions of the creeping flow equations around a circular cylinder. These, though, are for the total couple in a uniform shear field. No result is available for the local couple, as a function of l, in the case where shear rate varies along the particle axis. The effect of this couple for particles of large aspect ratio is relatively slight, except when the particle axis lies close to a plane of shear, when it is responsible for slow rotation across the streamline. In view of its limited importance, and the lack of a precise means for calculating its value, the shear-induced couple is therefore neglected in the present work. The consequence of this is that our results for rotation of finite aspect ratio particles in a shear flow show an asymptotic approach of the particle axis towards the plane of shear, behaviour that is only valid asymptotically for particles of very large aspect ratio.

The total couple on the particle is therefore written as follows and equated to zero for inertialess motion:

$$\mathbf{0} = \mathbf{p}\times\int_{-L}^{+L} \mathbf{f}l\,\mathrm{d}l = \mathbf{p}\times\int_{-L}^{+L} \mathbf{D}\cdot(\mathbf{v} - \mathbf{u}^{\mathrm{tr}} - \dot{\mathbf{p}}l)l\,\mathrm{d}l. \qquad [5]$$

For constant **D** it follows that

$$\dot{\mathbf{p}} = \frac{3}{2L^3}\int_{-L}^{+L} \mathbf{v}l\,\mathrm{d}l. \qquad [6]$$

This result for particle rotation was also obtained by Shanker *et al.* (1990).

The requirement for constant viscosity restricts the class of steady flows **v** that may be used in [4] and [6]. For more general flows, where viscosity varies through dependence on local shear rate, temperature etc., [2] and [5] must be used, and numerical integration will generally be needed. (It appears though, that Shanker *et al.* have used [4] and [6] in a variable viscosity planar shear flow with a complex velocity profile, as observed during injection moulding of a plastic.)

In the following sections we derive results for particle motion in some simple constant viscosity flows.

PLANAR SHEAR FLOWS

Consider flows of the form

$$v_1 = v_1(x_2), \quad v_2 = v_3 = 0. \tag{7}$$

It is convenient to express **p** in terms of Euler angles (figure 1), and we write

$$\dot{p}_\theta = \dot{\theta} = \frac{3}{2L^3}\int_{-L}^{L} v_\theta l \, \mathrm{d}l \tag{8a}$$

and

$$\dot{p}_\phi = \dot{\phi}\sin\theta = \frac{3}{2L^3}\int_{-L}^{L} v_\phi l \, \mathrm{d}l, \tag{8b}$$

where

$$\begin{aligned} v_\theta &= v_1 \sin\phi \sin\theta, \\ v_\phi &= v_1 \cos\phi, \\ x_2 &= l \sin\theta \cos\phi. \end{aligned} \tag{9}$$

The velocity field may be expressed in terms of an expansion about the particle centre, though for steady, constant viscosity flows, momentum conservation requires that derivatives of order 3 and higher are zero:

$$v_1(l) = \sum_{j=0}^{2} \frac{v_0^{(j)}}{j!}(l \sin\theta \cos\theta)^j, \tag{10}$$

where $v_0^{(j)}$ represents the jth derivative with respect to x_2 at $l = 0$. In transient flows higher order derivatives may exist, and we could extend [10] to represent an instantaneous velocity profile. In this way, the results that follow could also be extended, to give instantaneous velocities of rotation and translation in transient planar shear flows; in the following, however, we consider only steady flows.

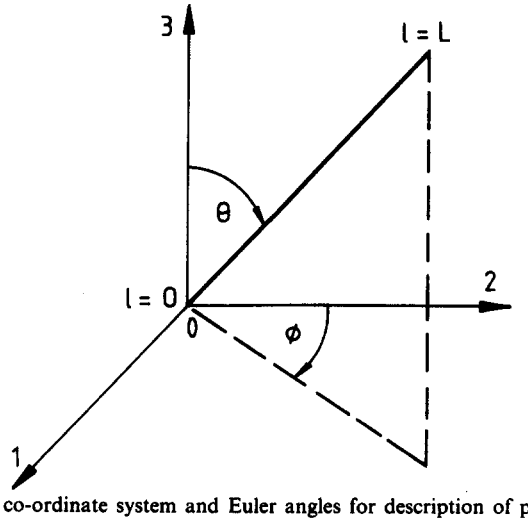

Figure 1. Cartesian co-ordinate system and Euler angles for description of particle orientation.

Using [4], it follows that

$$u_1^{tr} = \sum_{j=0}^{2} \frac{v_0^{(2j)}}{(2j)!} \frac{L^{2j}}{(2j+1)} (\sin\theta \cos\phi)^{2j}, \quad u_2^{tr} = u_3^{tr} = 0. \tag{11}$$

It is clear that in this class of flows, there is no motion of the fibre centre across streamlines, but slip along the streamline will occur in all flow fields other than the linear one.

From [8]–[10] the angular velocities are given as

$$\dot{\theta} = \sin\phi \cos\theta \sum_{j=0}^{2} \frac{v_0^{(2j+1)}}{(2j+1)!} \frac{3L^{2j}}{(2j+3)} (\sin\theta \cos\phi)^{2j+1} \tag{12a}$$

and

$$\dot{\phi} = \sum_{j=0}^{2} \frac{v_0^{(2j+1)}}{(2j+1)!} \frac{3L^{2j}}{(2j+3)} \sin^{2j}\theta \cos^{2j+2}\phi. \tag{12b}$$

We note that only even-order derivatives of the undisturbed fluid velocity are involved in determining the translational velocity, and only odd-order derivatives in the rotation.

Linear flow field

For

$$v_1 = \dot{\gamma} x_2, \quad v_2 = v_3 = 0, \quad \dot{\gamma} = \text{const}, \tag{13}$$

we have from [12a,b]

$$\dot{\theta} = \frac{\dot{\gamma}}{4} \sin 2\theta \sin 2\phi \tag{14a}$$

and

$$\dot{\phi} = \dot{\gamma} \cos^2\phi. \tag{14b}$$

These are to be compared with the results from Jeffery's (1922) theory, written with an equivalent ellipsoid axis ratio, r_e,

$$\dot{\theta} = \frac{r_e^2 - 1}{4(r_e^2 - 1)} \dot{\gamma} \sin 2\theta \sin 2\phi \tag{15a}$$

and

$$\dot{\phi} = \frac{\dot{\gamma}}{r_e^2 + 1} (r_e^2 \cos^2\phi + \sin^2\phi), \tag{15b}$$

which tend to the expressions derived here as $r_e \to \infty$ provided $\phi \neq \pi/2$. This is the expected behaviour, given the present use of the first approximation from slender body theory, and the neglect of shear-stress-induced couples.

As regards the translational velocity $\mathbf{u}^{tr}$, it is trivial to show that the particle centre moves with the velocity of the displaced fluid.

Quadratic flow field

Considering terms to the second order in [12a,b], it is apparent that the angular velocities are the same as for the linear case, [14a,b]. Integrating these with respect to time

$$\phi = \tan^{-1}(v_0^{(1)} t + c_1) \tag{16a}$$

and

$$\theta = \tan^{-1}(c_2 \sqrt{1 + (v_0^{(1)} t + c)_1^2}), \tag{16b}$$

where

$$c_1 = \tan \phi_i, \quad c_2 = \tan \theta_i \cos \phi_i;$$

θ_i and ϕ_i being the values at zero time. Taking terms up to second order in [11], and substituting from [16a,b], we integrate for the displacement of the particle centre:

$$\Delta x = v_0 t + \frac{v_0^{(2)}}{6v_0^{(1)}} \frac{L^2}{\sqrt{1+\frac{1}{c_2^2}}} \left[\tan^{-1}\left(\frac{v_0^{(1)} t + c_1}{\sqrt{1+\frac{1}{c_2^2}}} \right) - \tan^{-1}\left(\frac{c_1}{\sqrt{1+\frac{1}{c_2^2}}} \right) \right]. \quad [17]$$

The second term here represents the most interesting aspect of the motion in a quadratic flow field—slip of the particle centre along the streamline. To display this, it is convenient to introduce a dimensionless slipped distance:

$$\Delta x_s^* = \frac{\Delta x_s v_0^{(1)}}{L^2 v_0^{(2)}} = \frac{-1}{6\sqrt{1+\frac{1}{c_2^2}}} \left[\tan^{-1}\left(\frac{t^* + c_1}{\sqrt{1+\frac{1}{c_2^2}}} \right) - \tan^{-1}\left(\frac{c_1}{\sqrt{1+\frac{1}{c_2^2}}} \right) \right] \quad [18]$$

(i.e. if the particle centre falls behind the flow, then positive slip occurs); t^* is the dimensionless time $v_0^{(1)} t$.

Bearing in mind the definition of c_1 and c_2, it is clear that

$$\Delta x_s^* = F(\theta_i, \phi_i, t^*). \quad [19]$$

Space does not allow us to illustrate the dependence over a range of all three independent variables. Figure 2, however, shows one of the most interesting cases: the particle lies initially perpendicular to the streamlines, $\phi_i = 0°$, and rotates until it asymptotically approaches the streamline, $\phi = 90°$. The distance slipped during this rotation is plotted as a function of the release

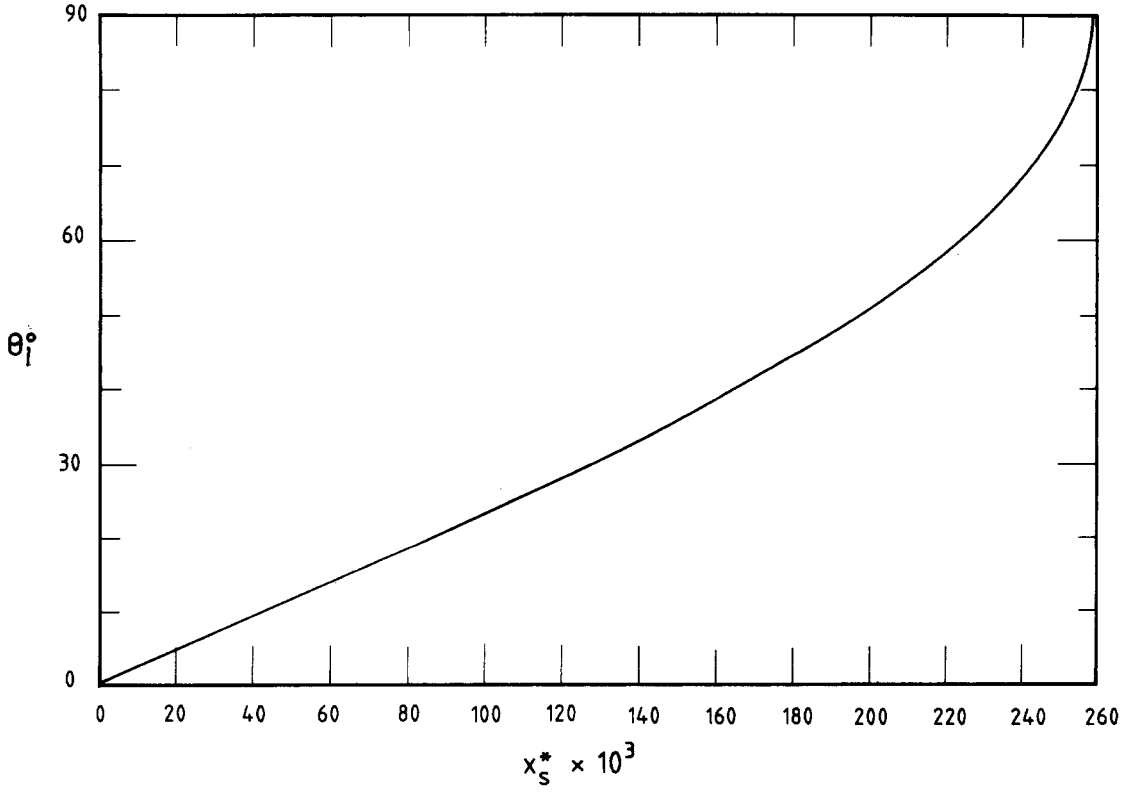

Figure 2. Dimensionless slipped distance, x_s^*, during rotation from $\phi = 0°$ to 90° in the quadratic flow as a function of the release angle θ_i.

angle θ_i. At $\theta_i = 0$, the particle lies in a plane of shear and does not slip. As θ_i increases, slip increases, and increases more rapidly as $\theta_i \to 90°$, with

$$\Delta x_s^* \to \frac{\pi}{12} \quad \text{as } \theta_i \to 90°. \tag{20}$$

Of course, ϕ approaches 90° only as $t^* \to \infty$, and the result above can be obtained by taking this limit in [18].

CYLINDRICAL SINK OR SOURCE FLOW

Analytic results for velocities of translation and rotation

Equations [4] and [6] are now applied to a rigid rod-like particle lying in the $r\theta$ plane of a cylindrical polar system, and experiencing the flow:

$$v_r = \frac{c}{r}, \quad v_\theta = v_z = 0. \tag{21}$$

Let the particle centre be instantaneously at radius r_0, and set up a Cartesian co-ordinate system with its origin at this point, see figure 3. The undisturbed fluid velocity at point l on the fibre axis has components referred to this system:

$$v_1(l) = \frac{c(r_0 + l \sin\phi)}{l^2 + r_0^2 + 2lr_0 \sin\phi} \tag{22a}$$

and

$$v_2(l) = \frac{cl}{l^2 + r_0^2 + 2lr_0 \sin\phi}. \tag{22b}$$

Substituting into [1] for the translational velocity, and integrating one obtains

$$u_1^{tr} = \frac{c}{4L}(\sin\phi \ln A + 2\cos\phi \tan^{-1} B) \tag{23a}$$

and

$$u_2^{tr} = \frac{c}{4L}(\cos\phi \ln A - 2\sin\phi \tan^{-1} B), \tag{23b}$$

where

$$A = \frac{\frac{L^2}{r_0^2} + 1 + 2\left(\frac{L}{r_0}\right)\sin\phi}{\frac{L^2}{r_0^2} + 1 - 2\left(\frac{L}{r_0}\right)\sin\phi}, \quad B = \frac{\frac{2L}{r_0}}{\left(1 - \frac{L^2}{r_0^2}\right)\sec\phi}.$$

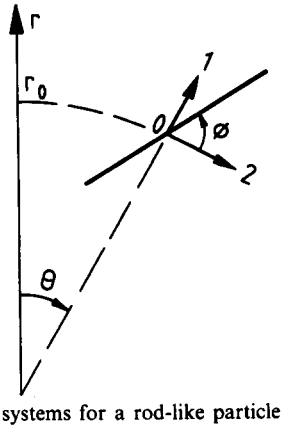

Figure 3. Geometry and co-ordinate systems for a rod-like particle in the cylindrical sink/source flow.

Defining the relative velocity of the particle centre along the streamline as

$$u_s = \frac{c}{r_0} - u_1^{tr} \qquad [24]$$

and scaling this by the undisturbed fluid velocity, c/r_0, at the current position of the fibre centre, the dimensionless relative velocity is written as

$$u_s^* = \frac{r_0}{c} u_s = 1 - \frac{1}{\frac{4L}{r_0}} (\sin\phi \ln A + 2\cos\phi \tan^{-1} B). \qquad [25]$$

In the present case, particle migration across the streamline is clearly also possible, and we have for the dimensionless migration velocity

$$u_2^* = \frac{r_0}{c} u_2^{tr} = \frac{1}{\frac{4L}{r_0}} (\cos\phi \ln A - 2\sin\phi \tan^{-1} B). \qquad [26]$$

To obtain the angular velocity, $\dot{\phi}$, we first need the ϕ-component of undisturbed fluid velocity at position l (see figure 3):

$$v_\phi(l) = \frac{c r_0 \cos\phi}{l^2 + r_0^2 + 2 l r_0 \sin\phi}. \qquad [27]$$

On substituting into the ϕ-component form of [6], the dimensionless angular velocity is given as

$$\dot{\phi}^* = \dot{\phi} \frac{r_0^2}{c} = \frac{3}{\frac{4L^3}{r_0^3}} (\cos\phi \ln A - 2\sin\phi \tan^{-1} B). \qquad [28]$$

It is clear that the dimensionless forms of the relative and migration velocities, and the angular velocity are all dependent on the instantaneous orientation ϕ and dimensionless particle position L/r_0 in the radial flow:

$$u_s^*, u_2^* \quad \text{and} \quad \dot{\phi}^* = F\left(\phi, \frac{L}{r_0}\right). \qquad [29]$$

The dependence of u_s^* on ϕ is shown in figure 4 with a family of curves having L/r_0 as parameter. As $L/r_0 \to 0$, $u_s^* \to 0$ for all ϕ; this can be shown by applying de l'Hôpitals rule to [25], or argued

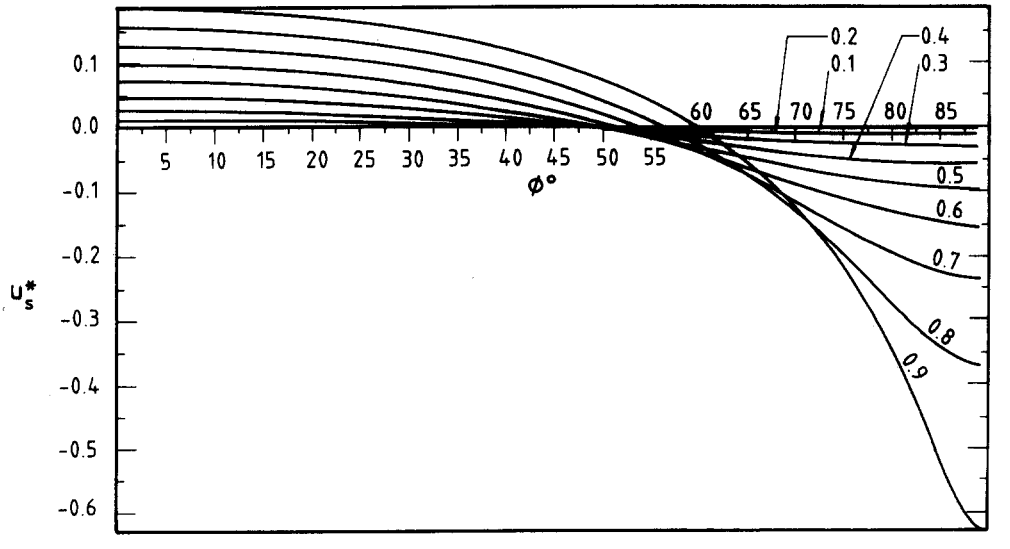

Figure 4. Dimensionless relative velocity along the streamline, u_s^*, vs particle orientation ϕ; parameter $L/r_0 = 0.1$ to 0.9.

on physical grounds by considering the fibre length to shrink to zero. For non-zero L/r_0, positive slip occurs at low values of ϕ and negative slip at values approaching 90°. The reasons for this can be understood by considering the variation of undisturbed fluid velocity along the length of the particle. For $\phi = 0°$, the particle lies perpendicular to the radial streamline through its centre and the fluid velocity here is greater than that at the particle ends. The mean fluid velocity experienced is therefore lower than the value at the centre, and the particle falls behind the flow, giving positive slip. The dimensional relative velocity increases more rapidly than the undisturbed fluid velocity as the particle approaches the flow sink. Thus, the dimensionless relative velocity u_s^* increases as L/r_0 increases. When $\phi = 90°$, the particle lies along a streamline, and as a consequence of the hyperbolic form of the velocity field, the mean velocity along the particle is greater than that at the centre point. The particle therefore moves ahead, giving negative slip. The dimensional relative velocity increases in magnitude more rapidly than the undisturbed flow as r_0 decreases; thus, u_s^* becomes more negative as L/r_0 increases. At intermediate values of ϕ it follows that the relative velocity passes through zero. The switch to negative values occurs at higher ϕ values for larger L/r_0.

One of the most interesting aspects of particle motion in the radial flow field is the occurrence of cross-streamline migration, a phenomenon never shown by rigid particles at low Reynolds number in unbounded parallel homogeneous flows. Figure 5 displays the dimensionless migration velocity, u_2^*, as a function of orientation ϕ, in a family of curves with parameter L/r_0. As with u_s^*, $u_2^* \to 0$ as $L/r_0 \to 0$ for all ϕ. It is clear that for $\phi = 0°$ and $\phi = 90°$ no migration will occur, and that the magnitude of u_2^* will attain a maximum at some intermediate orientation. As L/r_0 increases, the position of this maximum moves closer to $\phi = 90°$, and the magnitude of u_2^*, which is negative, increases. The physical interpretation of this is that for a source flow, $c > 0$ in [21], a particle lying in the $0° < \phi < 90°$ quadrant migrates in the positive O2 direction, see figure 3. If either the flow direction is reversed, or the particle lies in the $90° < \phi < 180°$ quadrant, the direction of migration is reversed.

Dimensionless angular velocity, $\dot{\phi}^*$, is shown as a function of ϕ and L/r_0 in figure 6. It can be shown from [29] that as $L/r_0 \to 0$, $\dot{\phi}^* \to -2 \sin\phi \cos\phi$. This is the result to be expected, as particle length tends to zero, and fluid velocity gradients over the particle tend to a constant. It was previously derived directly for this case by Harris & Pittman (1976). In this limiting case, the magnitude of $\dot{\phi}^*$ is a maximum at $\phi = 45°$, where it equals -1. As L/r_0 increases, the maximum shifts closer to $\phi = 90°$, and increases in magnitude. The behaviour is qualitatively similar to that shown by u_2^*—both types of motion being driven in a similar way by differences in magnitude and direction of the fluid velocity reactors at opposite ends of the particle. For a source flow, $c > 0$,

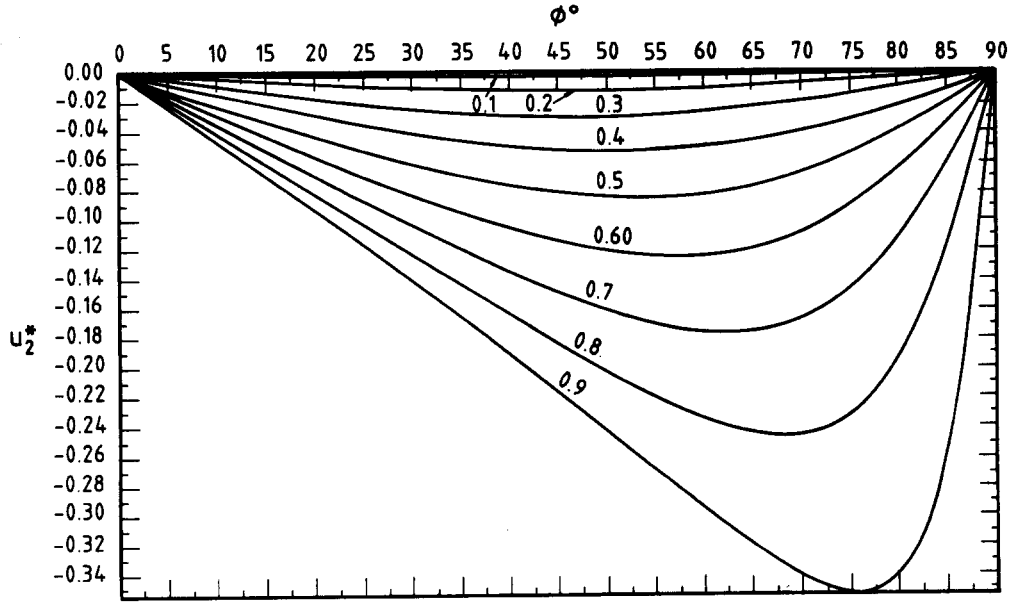

Figure 5. Dimensionless migration velocity across streamlines, u_2^*, vs particle orientation ϕ; parameter $L/r_0 = 0.1$ to 0.9.

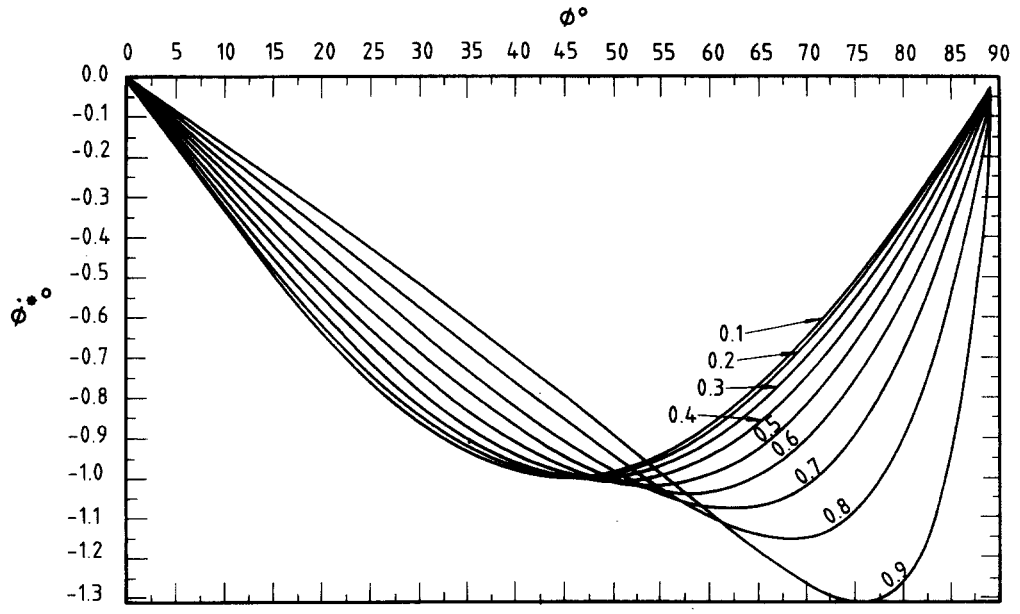

Figure 6. Dimensionless angular velocity, $\dot{\phi}^*$, vs particle orientation ϕ; parameter $L/r_0 = 0.1$ to 0.9.

the negative values of $\dot{\phi}^*$ correspond to rotation towards $\phi = 0°$, perpendicular to the streamline. Reversing the direction of flow, $c < 0$, of course brings about rotation towards $\phi = 90°$, and the approach to these limiting orientations is asymptotic. The effect of flow field inhomogeneity is thus seen to decrease the angular velocity at low ϕ, and increase it as $\phi \to 90°$.

Numerical results for displacement and orientation

The foregoing results for the relative, migration and rotation velocities have been integrated numerically using a computer program to evaluate the integrals in [4] and [6].

The particle length, $2L$, is divided into an even number of segments, N, of equal size, with nodes placed at the segment junctions and particle ends. For a given particle centre position and particle orientation, expressed in Euler angles (θ, ϕ), co-ordinates of the nodal points are calculated, referred to a Cartesian or polar co-ordinate system. A subroutine defining the undisturbed velocity field is entered with these co-ordinates and returns velocities $\mathbf{v}(l)$ at the nodes. The integrals are evaluated using Simpson's rule.

Particle displacements and orientation as a function of time are calculated by integrating $\mathbf{u}^{tr}$ and $\dot{\mathbf{p}}$ using the simple Euler method.

The programme was tested by ensuring precise agreement with a number of the analytic formulae that have been described. For the cases of interest, where no analytic results are available, thorough convergence studies were carried out, to determine satisfactory levels of particle length and time discretization. Details are given by Kasiri (1988). The accuracy in all the results displayed is greater than the precision of reading the graphs.

Dimensionless results for particle orientation, distance slipped and cross-streamline motion are presented in figure 7 as functions of particle centre displacement and time, in families of curves with parameter ϕ_i, the initial orientation. In all cases the ratio of particle half length L to initial particle centre position r_{0i} is 0.9. In these results, the distance slipped is scaled by r_{0i} and time by r_{0i}^2/c. These plots are now described; they may be used to provide quantitive information on particle motion for a wide variety of cases by entering the plots at appropriate points [see Kasiri (1988) for worked examples].

Figure 7(a) shows how the orientation ϕ changes, starting from various release values ϕ_i between 10° and 80°, as the particle centre moves outwards in the radial flow field ($c > 0$, [21]). Particle position is expressed in dimensionless form as the ratio of the current radial co-ordinate of the centre r_0 to the initial value r_{0i}. As r_0/r_{0i} increases, ϕ decreases asymptotically towards zero, as the particle tends to align along the principal strain axis of the fluid flow. The rate of change is more

rapid for larger ϕ_i, as expected from the results on angular velocity shown previously in figure 6. At $r_0/r_{0i} = 5$, $\phi < 9°$ for all release angles $10° \leqslant \phi_i \leqslant 80°$; and at $r_0/r_{0i} = 10$, $\phi < 2.5°$.

It is interesting to compare the particle rotation shown here with that predicted using homogeneous flow field theory. Using the assumption that velocity gradients are constant over the length of the particle, and equal to the values applying at the particle centre, Harris & Pittman (1976) obtained the following simple expression relating orientation to particle centre position:

$$\frac{\tan \phi}{\tan \phi_i} = \left(\frac{r_{0i}}{r_0}\right)^2. \qquad [30]$$

The corresponding curve (– – –) for a release angle $\phi_i = 80°$ is shown in figure 7(a). Rotation towards $Q = 0°$ is less rapid than when non-homogeneity is taken into account—the maximum difference being a lag of about 12° at $r_0/r_{0i} \approx 2.3$.

Figure 7(b) provides information on cross-streamline migration, in terms of changes in the angular position, $\delta\theta$, of the fibre centre (see figure 3), again as a function of r_0/r_{0i}, and with ϕ_i as parameter. The changes are initially rapid, with the largest changes corresponding to large ϕ_i, and settle to effectively constant values for $r_0/r_{0i} > 3$, as ϕ approaches low values [figure 7(a)]. This behaviour is understandable in view of the results on cross-streamline migration velocity already displayed in figure 5. It is interesting to note that the curve corresponding to $\phi_i = 80°$ lies below that for $\phi_i = 70°$ in figure 7(b); this is because, as shown in figure 6, the initial migration velocities for these cases (with $L/r_0 = 0.9$) lie on either side of the maximum in the migration velocity magnitude.

Figure 7(c) displays the dimensionless distance slipped along the streamline. For $\phi_i = 80°$, the relative velocity is initially negative, see figure 4, but changes sign as ϕ decreases. As a result, the slipped distance at first increases negatively, reaches a peak and then moves to positive values as r_0/r_{0i} increases. For release angle $\phi_i < 60°$, the slipped distance is always positive, increasing as ϕ_i decreases, corresponding to the higher relative velocities shown in figure 4 at low ϕ. Finally, figure 7(d) gives the fibre centre position $r_0 \leqslant r_{0i}$ as a function of dimensionless time, t^*. Here, curves for $10° \leqslant \phi_i \leqslant 80°$ almost superimpose, bringing out the point that slip along the streamline is relatively small in all cases.

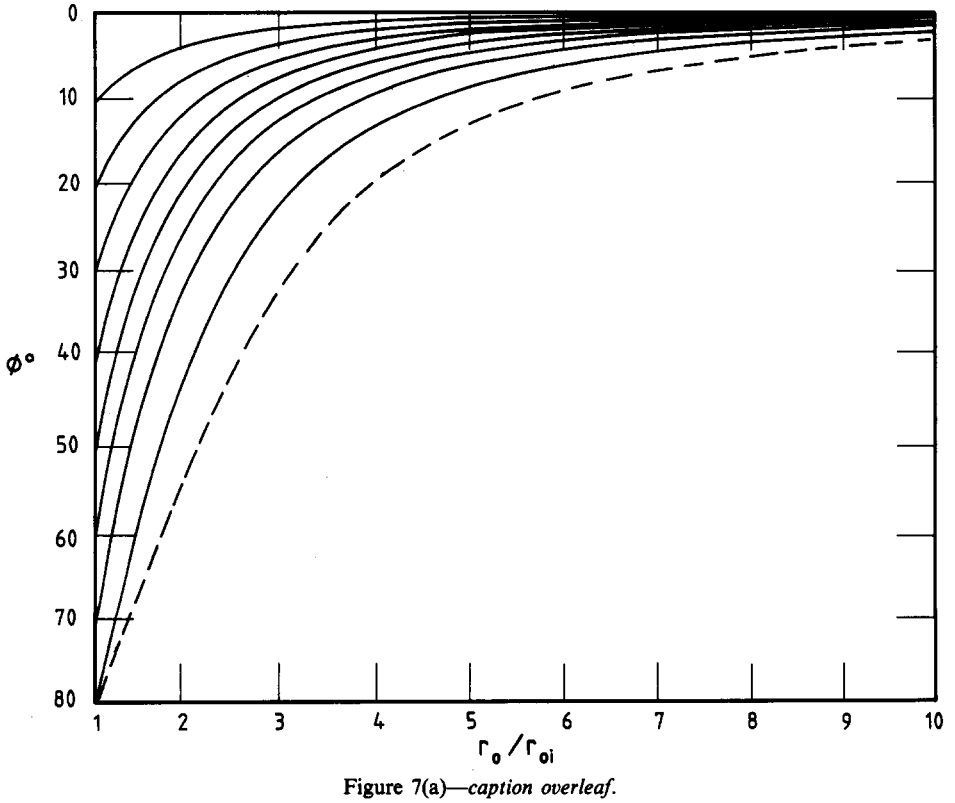

Figure 7(a)—*caption overleaf.*

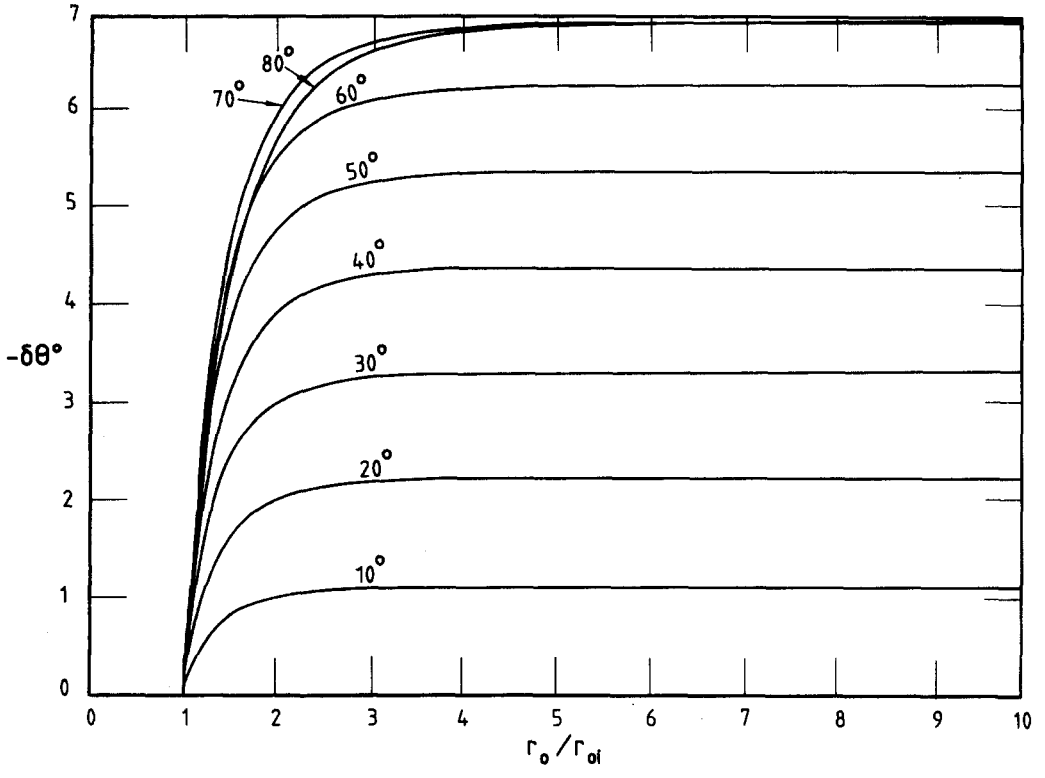

Figure 7(b)—*caption opposite.*

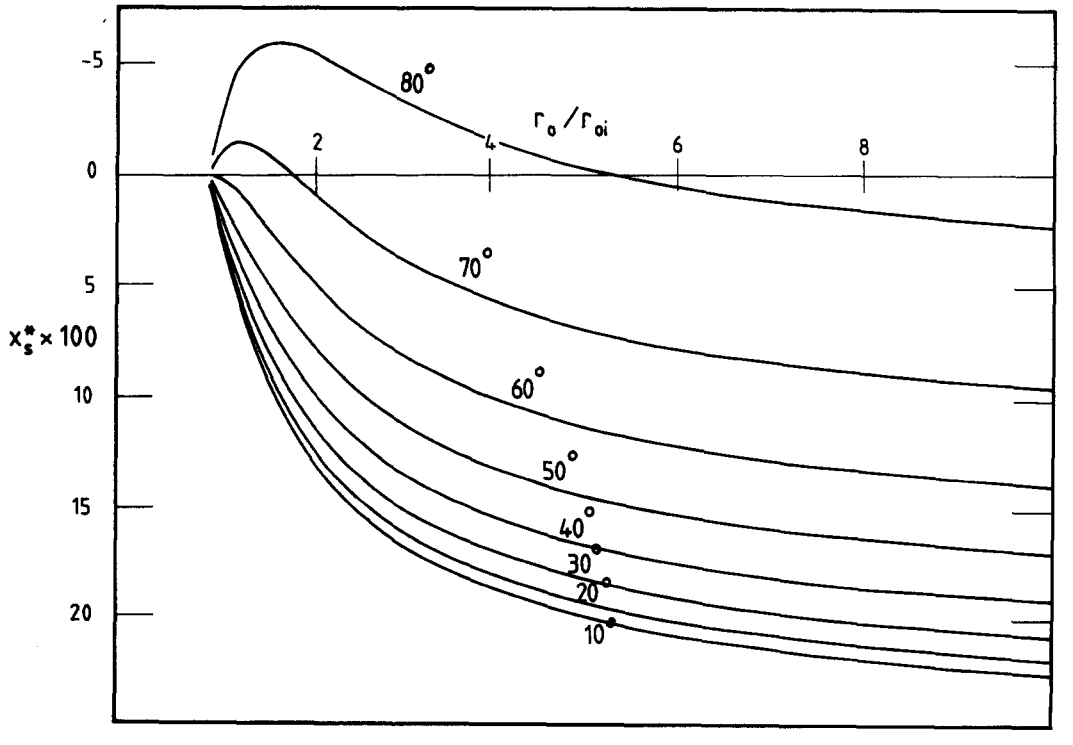

Figure 7(c)—*caption opposite.*

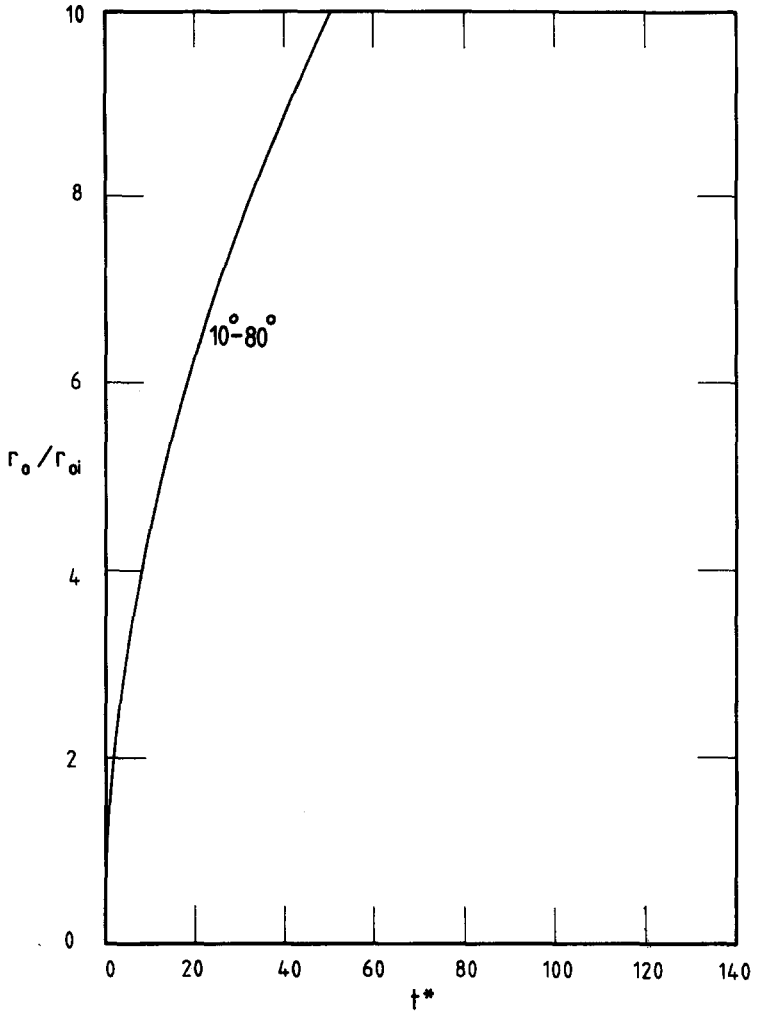

Figure 7(d)

Figure 7. Particle motion as a function of dimensionless instantaneous position of the particle centre r_0/r_{0i}. Dimensionless particle half length $L/r_{0i} = 0.9$ in all cases; parameter, release angle $\phi_i = 10°$ to $80°$. (a) Orientation ϕ—the dotted line is obtained from homogeneous flow theory, for $\phi_i = 80°$. (b) Cross-streamline migration in terms of change in angular position, $\delta\theta$, of the particle centre. (c) Dimensionless distance slipped along the streamline, x_3^*. (d) Dimensionless time, t^*.

CONCLUSION

General expressions have been derived for the motion of slender, rigid rod-like particles suspended in non-homogeneous Stokes flows and their validity and inherent simplifications discussed in some detail. Using simplified forms of these results a detailed study has been made of particle motion in some simple, steady, constant viscosity velocity fields. Where possible, analytic results for translation and rotation are derived, and in other cases solutions are obtained numerically, using a procedure capable of handling three-dimensional flows. Particle motion in planar Poiseuille and sink flows is displayed in terms of appropriate dimensionless quantities in a comprehensive set of plots, that conveniently provide quantitative information for a wide range of cases, for example, the differences in rotation and orientation arising from various degrees of inhomogeneity in the flow field, and the extent of slip along and across the streamlines. This information has not previously been available, and is of general interest in particle mechanics. It also has practical applications in estimating particle orientation produced by the given classes of flow, and in assessing the possibility of inhomogeneities developing in suspension concentration due to particle slip relative to the flow.

Acknowledgement—The computer programme used in this work was developed by Mahmoudzadeh (1990).

REFERENCES

BRENNER, H. 1964 The Stokes resistance of an arbitrary particle—3. Shear fields. *Chem. Engng Sci.* **19,** 631–651.

BRETHERTON, F. P. 1962 The motion of rigid particles in a shear flow at low Reynolds number. *J. Fluid Mech.* **14,** 284–304.

BRUNN, P. O. 1985 Linear polymers in nonhomogeneous flow fields. II. The cross-stream migration velocity. *J. Polym. Sci. Polym. Phys. Edn* **23,** 89–165.

COX, R. G. 1970 The motion of long slender bodies in a viscous fluid. Part 1. General theory. *J. Fluid Mech.* **44,** 791–810.

COX, R. G. 1971 The motion of long slender bodies in a viscous fluid. Part 2. Shear flow. *J. Fluid Mech.* **45,** 625–657.

DINH, S. M. & ARMSTRONG, R. C. 1984 A rheological equation of state for semi-concentrated fibre suspensions. *J. Rheol.* **28,** 207–227.

FOLGAR, F. & TUCKER, C. L. III 1984 Orientation behaviour of fibres in concentrated solutions. *J. Reinforced Plastics Composites* **3,** 98–119.

GIESEKUS, H. 1962 Strömungen mit Konstanten Geschwindigkeitsgradienten und die Bewegung von darin Suspendierten Teilehen. *Rheol. Acta* **2,** 101–112.

GILLESPIE, J. W. JR, VANDERSCHUREN, J. A. & PIPES, R. B. 1985 Process induced fibre orientation. Numerical simulation, with experimental verification. *Polym. Composites* **6,** 82–86.

GIVLER, R. C., CROCHET, M. J. & PIPES, R. B. 1982 Numerically predicted fibre orientation in dilute suspensions. In *Numerical Methods in Industrial Forming Processes*; *Proc. Int. Conf., Swansea* (Edited by PITTMAN, J. F. T., WOOD, R. D., ALEXANDER, J. M. & ZIENKIEWICZ, O. C.), pp. 559–576. Pineridge Press, Swansea, Wales.

GOLDSMITH, H. L. & MASON, S. G. 1967 The microrheology of dispersions. In *Rheology*, Vol. 4 (Edited by EIRICH, F. R.). Academic Press, New York.

HARRIS, J. B. & PITTMAN, J. F. T. 1976 Alignment of slender rod-like particles in suspension using converging flows. *Trans. Instn Chem. Engrs* **54,** 73–83.

JACKSON, W. C., FOLGAR, F. & TUCKER, C. L. III 1984 Prediction and control of fibre orientation in molded parts. In *Polymer Blends and Composites in Multi Phase Systems* (Edited by HAN, C. D.); *Adv. Chem. Ser.* **206,** 279–299.

JEFFERY, G. B. 1922 The motion of ellipsoidal particles immersed in a viscous fluid. *Proc. R. Soc.* **A102,** 161–179.

JHOU, M. S. 1985 Polymer migration in Newtonian fluids. *J. Polym. Sci. Polym. Phys. Edn* **23,** 955–971.

KASIRI, N. 1988 Fibre motion in non-linear flow fields. M.Sc. Thesis, Dept of Chemical Engineering, Univ. of Swansea, Wales.

LIPSCOMBE, G. G. II, DENN, M. M., HUR, D. U. & BOGER, D. V. 1988 The flow of fibre suspensions in complex geometries. *J. Non-Newton. Fluid Mech.* **26,** 297–325.

MAHMOUDZADEH, H. 1990 Flow and orientation in fibre-loaded resins. Ph.D. Thesis, Univ. College, Swansea, Wales.

SALARIYA, A. K. & PITTMAN, J. F. T. 1990 Preparation of aligned discontinuous fibre pre-pregs by deposition from suspension. *Polym. Engng Sci.* **20,** 787–797.

SHANKER, R., GILLESPIE, J. W. JR & GÜÇERI, S. I. 1990 Rheology of fibre suspensions in nonhomogeneous flow fields. Translation induced effects. Presented at the *ASME Winter A. Mtg*, Dallas, TX.

SHANKER, R., GILLESPIE, J. W. JR & GÜÇERI, 1991 On the effect of nonhomogeneous flow fields on the orientation distribution and the rheology of fibre suspensions. *J. Polym. Engng Sci.* **31,** 161–172.

TAYLOR, G. I. 1923 The motion of ellipsoidal particles in a viscous fluid. *Proc. R. Soc.* **A103,** 58–61.

TUCKER, C. L. III 1984 Compression molding of polymers and short fiber composites. In *Injection and Compression Molding Fundamentals* (Edited by ISAYEV, A. I.). Marcel Dekker, New York.

VINCENT, M. & AGASSANT, J. F. 1985 Experimental and theoretical study of short fibre orientation in diverging flows. *Rheol. Acta* **24,** 603–810.

YOUNGREN, G. K. & ACRIVOS, A. 1975 Stokes flow past a particle of arbitrary shape: a numerical method of solution. *J. Fluid Mech.* **69,** 377–403.